Impact of Alternative Fuels on the Operational and Environmental Performance of Commercial Aircraft

Ricardo Manuel Pereira Gaspar
ricardomgaspar@ist.utl.pt

Instituto Superior Técnico, Lisboa, Portugal

July 2016

Abstract

The wide-scale supply of sustainable alternative fuels has become a major element of the aviation industry's aim of reducing environmental impacts while easing fossil fuels dependence. The present work will address the technical feasibility of a wide range of alternative fuels, with differences in performance and pollutant emissions summarized. The alternative production pathways considered in this study are the following: Fischer-Tropsch, Hydrotreated Esters and Fatty Acids, Synthesized Iso-Paraffins, Alcohol-to-Jet, Catalytic Hydrothermolysis and Hydrodeoxygenation. The analysis of the burning of different fuels will be based purely on a 0-D engine thermodynamic approach, with a numerical modelling of a typical two-spool turbofan for off-design and transient simulations. Through comparison of performance results obtained relative to what would be obtained with GasTurb 12, for a conventional kerosene, the aero-engine numerical model is validated. The approaches followed, for the estimation of required fuel properties and flame temperatures and for the implementation of evaporation and gas models, are presented and validated. For different flight conditions, performance and pollutant emissions outputs for the fuels studied are presented, discussed and compared with results obtained in the literature. Finally, different transient scenarios are simulated and the influence of fuels analysed. With the present work, it is possible to conclude that most sustainable alternative fuels may improve the overall performance and pollutant emissions when compared with a conventional kerosene, which confirms that the supply of alternative fuels, although constrained economically, is a safe route going forward for the aviation industry.

Keywords: Alternative Fuels, Turbofan, Off-Design Performance, Transient Response, Pollutant Emissions

1. Introduction

Being the only anthropogenic source of pollutant emissions in the lower stratosphere and upper troposphere, a major challenge for the aviation industry is the need to reduce its share of environmental air pollution. In fact, in 2010, at the 37^{th} Session of ICAO Assembly, ICAO Member States adopted collective global aspirational goals for the international aviation sector to improve annual fuel efficiency by 2%, and to limit CO_2 emissions at 2020 levels, reaching a carbon-neutral growth (CNG2020), relative to 2005 [1].

The need for constant improvements in engine performance when associated with the need to decrease pollutant emissions is a complex subject. To achieve this goal, the Sustainable Alternative Fuels (SAF) route is viewed as a key element, along with technological and infrastructural improvements. Since mid-2009, a growing interest on SAF has been verified.

The worldwide supply of alternative fuels in the aviation industry would present additional advantages, such as the ease in petroleum dependence, that is depleting, the economical development in different regions of the world and the fact that changes in aircraft or infrastructures are not required ("drop-in" fuels). On the other hand, the fuel production must not compete with food production, neither cause land-use change effects such as deforestation. The biggest challenge for the successful growth of alternative fuels is mainly economical and political [2].

At the moment of the writing of the present work, five production pathways are already ASTM approved: Fischer-Tropsch (FT-SPK) in 2009; Hydrotreated Esters and Fatty Acids (HEFA-SPK) in 2011; Synthesized Iso-Paraffins (SIP) in 2014; Fischer-Tropsch Synthetic Kerosene with Aromatics (FT-SKA) in 2015; and Alcohol-to-Jet (ATJ-SPK) in 2016. With SPK standing for Synthetic Paraffinic Kerosene. The maximum volume blending ratios approved were of 50% for FT and HEFA-

SPK, of 30% for ATJ-SPK and of 10% for SIP.

In terms of composition (paraffinic and aromatic), most production pathways being developed, supply jet fuels with low aromatic content when compared with conventional kerosene, which is why there is a growing aim for synthetic kerosenes with aromatics. Fuel properties such as the liquid density, the viscosity, the surface tension and the normal boiling point have a significant impact on fuel atomization and evaporation which ultimately has an impact on the combustion efficiency [3].

Changes in pollutant emissions are also dependent on fuel properties. With a typical increase in combustion chamber's temperatures, NO_x pollutant emissions are the most undesired of the aviation industry. Along with these, CO, UHC and soot (smoke) pollutant emissions are also regulated by ICAO. Although accurate estimations are highly complex (mainly for UHC and soot emissions), in a numerical approach, with good results, empirical correlations are usually followed, as in the work of Rizk and Mongia [4].

The overall performance of an aircraft engine can be typically defined by its thermodynamic cycle analysis. Due to its simplicity, low computational demand and accurate results obtained, a 0-D model will be followed for all thermodynamic analyses: design point, off-design and transient analyses. Typically, the design point of an engine may be defined in a high power operating condition. Then, through turbofan spool work balances, polytropic compression and expansion processes and separate nozzles exhaust gases conditions, the engine behaviour at design point is properly defined. Engine performance at different operating conditions may, then, be evaluated through an off-design analysis. For a complete analysis of a given engine performance, response to transient engine demands should also be evaluated.

Different approaches may be followed, mostly in respect to: the gas model implemented; the use of component maps or assumption of fixed selected engine parameters, in off-design; or an iterative constrain approach instead of a rapid inter-component volume method, ICV, for transient simulations. Multi-variable iterative methods are usually required, with the Newton-Raphson method being a common approach in such calculations. The proper implementation of the turbofan model is mostly based on references [5, 6, 7] and detailed in section 3.

The main goal of the present work is to numerically analyse the impact of the combustion of different fuels on the performance and pollutant emissions of a typical turbofan. For that purpose, a 0-D two-spool turbofan thermodynamic model (design, off-design and transient) is to be implemented in MATLAB. With a quantification of fuel properties influence on atomization, evaporation and flame temperature results, an overview of a wide-range of alternative fuels and respective impact on performance and exhaust emissions of an aircraft is given.

2. Sustainable Alternative Fuels

Along with the required study of a conventional civil aviation turbine fuel, i.e. Jet A-1, which is defined by ASTM D1655 specification limits (ASTM D7566 for alternative fuels certification), ten types of alternative fuels varying in feedstock and/or production process were selected for the present work, as presented in Table 1, with properties obtained in the literature. It should be highlighted that, although GTL and CTL are not sustainable fuels (fossil fuel dependence), with lack of information on BTL (FT from biomass) and assumed similar fuel properties (same refining process), their study is relevant.

Designation	Feedstock	Pathway
CTL	Coal	FT-SPK
GTL	Natural Gas	
HEFA R-8	Mixed Fats	HEFA-SPK
HEFA Camelina	Camelina Oil	
CH	Carinata Oil	CH
ATJ-SPK	Corn	ATJ-SPK
ATJ-SKA	Biomass	ATJ-SKA
SIP	Sugars	SIP
HDO-SK	Biomass	HDO-SK
Green Diesel	Vegetable Oil	HEFA

Table 1: Fuels of interest.

The production pathways mostly differ on feedstock and on relevant productions steps. Fuels produced from FT-SPK pathway are based on the conversion of syngas into liquid hydrocarbons with a Fischer-Tropsch synthesis, presenting a wide range of feedstock possibilities such as coal, natural gas, wastes or lignocellulosic biomass. With HEFA-SPK production, through hydroprocessing and from vegetable or waste oils, jet fuels are produced. For the ATJ production pathway, alcohol synthesis is required from feedstock such as sugars and starches, which are then thermoprocessed. SIP jet fuel (mostly farnesane) is mostly produced through sugar fermentation. With similar type of feedstock compared to HEFA, the HDO-SK fuel production requires an hydrodeoxygenation step. In the CH pathway, a catalytic hydrothermolysis is required, with feedstock ranging from sugars and starches to lignocellulosic biomass. Green Diesel is a blending

approach, produced from the HEFA process [8].

From their composition analysis it becomes evident an overall lack of aromatics when comparing with Jet A-1. Those most similar in composition, from the ones studied, are the CH and ATJ-SKA. In a life cycle greenhouse gas emissions analysis, it is proven that although indirect land use change (among others) must be carefully accounted for, there's an overall improvement in life cycle emissions with all alternative pathways. In fact, researches results showcase that, in general, the decrease in greenhouse gases emissions can be greater than 50% in a life cycle perspective, when compared with conventional production. However, as previously stated, this route is still considered an expensive product, dependent on crude oil prices. Nevertheless, it is expected that, with higher energy demand and petroleum depletion, the conventional jet fuel price will steadily increase, while an expected maturation of alternative fuels shall lead to a decrease in alternative fuel prices.

3. Implementation

The main implementation goal, in the present work, is to thermodynamically model a typical two-spool turbofan in a 0-D approach. The aero-engine will be defined with the implementation of a diffuser followed by a low-pressure compressor (LPC), a high-pressure compressor (HPC), a combustion chamber (burner), a high-pressure turbine (HPT), a low-pressure turbine (LPT) and a convergent core nozzle, through the core of the engine. Being a turbofan, the bypass air mass flow (cold flow) will run through the fan and the convergent bypass (or fan) nozzle. This type of turbofan and station numbering is schematically presented in Figure 1.

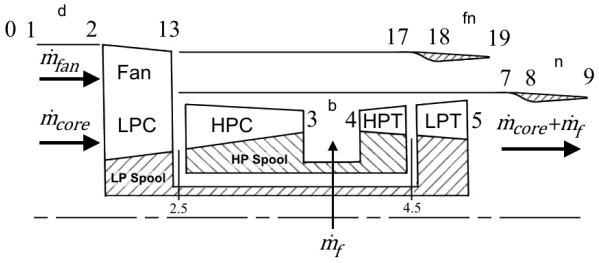

Figure 1: Two-spool turbofan station numbering ([9], adapted).

It is required that all fuel properties (for each fuel of interest) are read in the beginning of each calculation. In this regard, values of liquid fuel density at 15^oC, viscosity at two different temperatures, net heat of combustion (ΔH), hydrogen mass content ($H\%$), hydrogen-to-carbon ratio, molecular weight and distillation range are read for each fuel. Then, for cases where a certain fuel property is unknown and for estimations at different temperatures, correlations used for petroleum fractions, such as in [10], are assumed for alternative fuels. With this approach additional important results such as critical properties or the surface tension are estimated. The results obtained are then validated with measured properties in the literature. The modelling of fuel properties is completed with the implementation of a blending option, where properties of a given fuel and those of Jet A-1 are compared for a certain volume blend ratio.

For an accurate simulation of fuel effects on combustion, the impact of fuel properties on the flame temperature [11] as well as on the droplet evaporation rate [12], are modelled and validated, based on results available in the literature. It should be pointed out that the evaporation model assumes (quasi) steady-state evaporation, which for higher burner ambient pressures than those critical for a given fuel (p_{cr}) and high flame temperatures becomes mostly transient. For such cases, the present model assumes a maximum evaporation rate at the fuel critical pressure, as an approximation.

3.1. Design Point Model

The design point modelling follows the conventional approach given in the literature [6, 9]. The main differences arising from the fact that, for increased accuracy, a variable specific heat model is considered (based on [13]) as well as the influence of atomization and evaporation on design combustion efficiency, $\eta_{b,R}$, quantified:

$$\frac{1-\eta_{b,R}}{1-\eta_{b,R,ref}} = \left(\frac{\lambda_{ref}}{\lambda}\right) \cdot \left(\frac{D_0}{D_{0,ref}}\right)^2, \qquad (1)$$

where, λ is the evaporation constant (defining evaporation rate), D_0 the initial droplet diameter and subscript ref referring to Jet A-1.

Based on the work of Lefebvre [3], the ratio of drop diameters, $D_0/D_{0,ref}$, for pressure-swirl atomizers, may be computed based on liquid dynamic viscosity, μ_F, and surface tension, σ_F:

$$\frac{D_0}{D_{0,ref}} = \left(\frac{\sigma_F}{\sigma_{F,ref}}\right)^{0.25} \cdot \left(\frac{\mu_F}{\mu_{F,ref}}\right)^{0.25}. \qquad (2)$$

The calculation of the evaporation constant, λ, required for equation 1, is based on the (quasi) steady-state evaporation model followed.

In order to compute the design point (required for off-design simulations), several design inputs are necessary, being the most relevant those presented in Table 2.

Whereas efficiencies (polytropic, e, and mechanical, η_m) and pressure losses may be assumed based on a given Level of Technology [6], design values (subscript R) for flight Mach number, M_0, and altitude, H, engine inlet mass flow rate, $\dot{m}$

Flight Data	Burner Design
$M_{0,R}$, H_R	T_f, q_{pz}, q_{sz}
Efficiencies	**Engine Design**
e_{fan}, e_{LPC}, e_{HPC}, e_{HPT}, e_{LPT}, $\eta_{b,R,ref}$, $\eta_{m,L}$, $\eta_{m,H}$	$\dot{m}_R$, B_R, $T_{t4,R}$, $\pi_{fan,R}$, $\pi_{LPC,R}$, $\pi_{HPC,R}$
Pressure Losses	
$\pi_{b,R}$, $\pi_{n,R}$, $\pi_{fn,R}$	$N_{L,R,abs}$, $N_{H,R,abs}$

Table 2: Engine design point inputs.

User inputs	H, M_0		
	N_L	N_H	T_{t4}
Input-dependent Iteration Variables	T_{t4}	T_{t4}	N_L
	N_H	N_L	N_H
Fixed Iteration Variables	β_{LPC}, β_{HPC}, β_{HPT}, β_{LPT}, B		

Table 3: Off-design user inputs and iteration variables.

($\dot{m}_{core} + \dot{m}_{fan}$), bypass ratio, B, high-pressure turbine inlet total temperature, T_{t4}, fan and compressors pressure ratios, π_{fan}, π_{LPC} and π_{HPC}, fuel initial temperature, T_f, and combustion chamber's primary and secondary zones air fraction employed, respectively q_{pz} and q_{sz}, must be defined, based on engine requirements.

Design absolute spool speeds, $N_{L,R,abs}$ and $N_{H,R,abs}$, should also be defined for off-design and transient calculations.

At the end of a certain design point calculation, all station mass flow rates, total temperatures and pressures (T_t and p_t, respectively) as well as nozzles fixed areas, are computed and saved. For the scope of this work, the outputs considered as the most relevant are the total thrust, F, and the specific fuel consumption, SFC, where

$$SFC = \frac{\dot{m}_f}{F}.10^6 \text{ g/kN.s} , \qquad (3)$$

with the fuel mass flow rate, $\dot{m}_f$, given in kg/s and F given in N. In this regard, the calculation of the fuel-air ratio, f (kg of fuel/kg of air), is of major relevance throughout this work.

3.2. Off-Design Model

Off-design calculations are performed to simulate a given engine performance behaviour at different operating conditions. This may be achieved with the variation of the flight data (altitude and Mach number), with variation of T_{t4} or through changes in engine relative (to design) spools speeds, N_L and N_H, respectively the low-pressure and high-pressure relative spool speeds (Table 3).

The off-design numerical model assumed in the present work follows, mostly, the work of Kurzke [7]. For a certain component inlet corrected mass flow rate and corrected relative spool speed, values of pressure ratio across the component and adiabatic isentropic efficiency are computed. This relationship between referred parameters is defined with the construction of a component map (Figure 2). For ease in map reading, auxiliary map coordinates, β, are defined between 0 and 1 (surge line).

It follows that, for a given component inlet state i, nondimensional total temperatures, θ_i, and pressures, δ_i, must be calculated:

$$\theta_i = \frac{T_{ti}.R_i}{T_{SL}.R_{SL}}, \qquad (4) \qquad\qquad \delta_i = \frac{p_{ti}}{p_{SL}}, \qquad (5)$$

with T_{SL}, p_{SL} and R_{SL} the temperature, pressure and dry air gas constant at sea level ISA conditions.

Then, corrected mass flow rates $\dot{m}_{i,corr}$ and corrected relative spool speed, N_x, (for a component x) are given by

$$\dot{m}_{i,corr} = \dot{m}_i.\sqrt{\theta_i}/\delta_i, \qquad (6)$$

$$N_x = N_{L(H)}.\sqrt{\frac{\theta_{i,R}}{\theta_i}}. \qquad (7)$$

In the present work, component maps available with [7] are used, requiring a simple scaling process for design point matching.

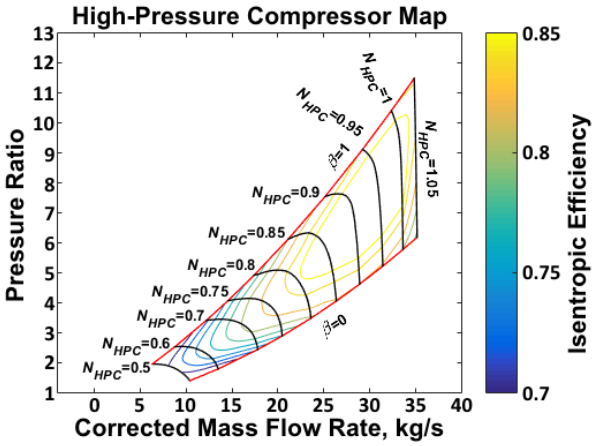

Figure 2: High-pressure compressor unscaled map. Based on data from [7].

With calculated corrected mass flow rates and relative spool speeds, a multi-variable Newton-Raphson iterative method, with 7 iteration variables (Table 3) for 7 iteration errors, is considered. As in [7], work and flow compatibility is assumed, as well as fixed convergent nozzles cross section areas.

Ultimately, desired outputs such as SFC or new values of B or T_{t4}, for example, can be computed for a given set of user inputs.

3.3. Transient Model

In the present work, the transient modelling completes the thermodynamic implementation of the turbofan. With this model, and taking into account the main goal of this work, it is important to verify if alternative fuel burning may induce engine transient response delays, compromising flight safety.

As for the off-design model, with an accurate validation of the model in mind, the work of Kurzke [7] is followed. The transient model shall enable acceleration and deceleration operating conditions.

The user must define the time-dependent, t, demands, which can be a direct fuel mass flow rate injection, $\dot{m}_{f,demand}(t)$, a power setting, $P_{demand}(t)$ in %, or total thrust, $F_{demand}(t)$, demands, as in Table 4. It becomes relevant to highlight that in the present model, power setting is directly related to the low-pressure relative spool speed, $N_{L,demand}(t)$.

For power setting or thrust demand, a conventional PID (Proportional-Integral-Derivative) controller is used, so that knowing computed values of $N_L(t)$ or $F(t)$ and correspondent demanded values, $N_{L,demand}(t)$ or $F_{demand}(t)$, an increase or decrease in fuel mass flow rate input is calculated.

User inputs	
Initial Conditions (Off-Design)	H, M_0
	N_L, N_H or T_{t4}
Transient inputs	$\dot{m}_{f,demand}(t)$
	$P_{demand}(t)$
	$F_{demand}(t)$
Iteration Variables	
β_{LPC}, β_{HPC}, β_{HPT}, β_{LPT}, B, T_{t4}	

Table 4: Transient user inputs and iteration variables.

In short, the main difference between transient and steady-state simulations, is the fact that for transient calculations, differences between the power required for compression and the turbine power generated, will lead to a spool acceleration or deceleration. For the present case, high-pressure and low-pressure spool speed accelerations, dN_H/dt and dN_L/dt respectively, in RPM/s, are given by

$$\frac{dN_H}{dt} = \frac{\left(\frac{60}{2\pi}\right)^2.(\dot{W}_{HPT} - \dot{W}_{HPC})}{I_H.N_{H,abs}}, \tag{8}$$

$$\frac{dN_L}{dt} = \frac{\left(\frac{60}{2\pi}\right)^2.(\dot{W}_{LPT} - \dot{W}_{LPC} - \dot{W}_{fan})}{I_L.N_{L,abs}}, \tag{9}$$

with $\dot{W}_x$ given in power units W (with x defining a component) and I_H and I_L, the spools moment of inertia, in kg.m^2. The turbine power available takes into account the spool mechanical efficiency.

With computed spool accelerations, new values of spool speeds for the next simulation time are computed. In the present work, an explicit integration method is considered, for simplicity of numerical implementation.

For each transient simulation time, a numerical procedure similar to the one followed in the off-design model is implemented. Here, a multivariable Newton-Raphson iterative method with 6 iteration variables (Table 4) for 6 iteration errors is considered. Flow compatibility, fixed convergent nozzles cross section areas and a fuel mass flow rate input are assumed. Output parameters calculated (same as in off-design) are then presented as a function of time, t.

3.4. Pollutant Emissions Model

Based on [4], emissions of oxides of nitrogen, NO_x, carbon monoxides, CO, unburned hydrocarbons, UHC, and soot (smoke) are analysed. NO_x, CO and UHC pollutant emissions are quantified by the respective emission index, EI in g of emitted substance/kg of fuel and soot exhaust concentration, S, in mg of emitted substance/kg of exhaust gas:

$$EI_{NO_x} = \frac{1.5\times10^{15}.\sqrt{\tau-0.5\tau_e}.e^{\frac{-71000}{T_{st}}}}{p_{t3}^{0.05}.\sqrt{\frac{\Delta p_{t3}}{p_{t3}}}}, \tag{10}$$

$$EI_{CO} = \frac{1.8\times10^{8}.e^{\frac{7800}{T_{pz}}}}{p_{t3}^{2}.\sqrt{\frac{\Delta p_{t3}}{p_{t3}}}.(\tau-0.4\tau_e)}, \tag{11}$$

$$EI_{UHC} = \frac{7.6\times10^{10}.e^{\frac{9756}{T_{pz}}}}{p_{t3}^{2,3}.\left(\frac{\Delta p_{t3}}{p_{t3}}\right)^{0.6}.(\tau-0.35\tau_e)^{0.1}}, \tag{12}$$

$$S = 0.0145\times\frac{f_{pz}.\left(\frac{p_{t3}}{1000}\right)^2}{q_{pz}.\dot{m}_3.T_{pz}}\times(18-H\%)^{1.5} \times\left(1-0.00515\frac{e^{0.001T_{sz}}}{f_{sz}}\right), \tag{13}$$

with p_{t3} and $\Delta p_{t3} = p_{t3} - p_{t4}$ in Pa, $\dot{m}_3$ in kg/s and the hydrogen content, $H\%$, in weight %.

Temperatures T_{st} and T_{pz}, in K, are to be calculated with the flame temperature model, for stoichiometric, f_{st}, and primary zone, f_{pz}, fuel-air ratios, respectively. The secondary zone temperature, T_{sz}, is, as an approximation, obtained as an average value between T_{pz} and T_{t4}, weighted by air fractions (q_{pz} and q_{sz}).

Since actual combustion evaporation times, τ_e, given in s, are highly dependent on an accurate initial drop diameter calculation, its computation will be performed from a minimum value of zero (infinitely fast evaporation) to the combustion residence time, τ, given in s. The evaporation time required for Jet A-1 evaporation, $\tau_{e,ref}$, will be varied assuming full evaporation in the primary zone, for a fixed selected residence time, τ_{ref}. Each value of reference residence and evaporation time is then compared to what would be obtained for a different fuel with equations 14 and 15, respectively:

$$\tau = \tau_{ref}.\frac{p_{t3}.\dot{m}_{3,ref}.T_{pz,ref}}{p_{t3,ref}.\dot{m}_{3}.T_{pz}}, \tag{14}$$

$$\tau_e = \tau_{e,ref}.\left(\frac{D_0}{D_{0,ref}}\right)^2.\left(\frac{\lambda_{ref}}{\lambda}\right). \tag{15}$$

With this approach, a range of results will be obtained for the condition that both analyses (Jet A-1 and an alternative fuel emissions with evaporation time) are conducted considering complete fuel evaporation in the primary zone for both fuels ($\tau_e < \tau$ and $\tau_{e,ref} < \tau_{ref}$). Then, differences in NO_x, CO and UHC pollutant emissions, relative to those obtained with Jet A-1, will be computed with average, maximum and minimum estimations.

4. Results

In the present work, the design point flight condition considered is the Top of Climb, defined by a flight Mach number of $M_{0,R} = 0.8$ and altitude of $H_R = 10668$ m. It is considered that, in the design point, the relative spool speeds are equal to 1 and engine component auxiliary coordinates, β_R, equal to 0.5.

In the design point selection, it is considered an engine with $T_{t4,R} = 1550$ K, $\pi_{fan,R} = 1.7$, $\pi_{LPC,R} = 2$, $\pi_{HPC,R} = 6$, $B_R = 5.7$ and $\dot{m}_R = 100$ kg/s. Remaining parameters such as component efficiencies and pressures losses (Table 2) are defined by a Level of Technology 3 [6]. Additionally, mostly for pollutant emissions calculations, design combustion chamber parameters were selected, with $T_f = 298.15$ K, $q_{pz} = 0.35$ and $q_{sz} = 0.6$. For off-design and transient calculations, design point absolute spool speeds are also defined with $N_{H,R,abs} = 13500$ RPM and $N_{L,R,abs} = 10000$ RPM. Exclusively for transient calculations, spools polar moments of inertia are also required, being selected $I_L = 2$ kg.m^2 and $I_H = 3$ kg.m^2.

For different fuel burning analysis, different flight conditions of interest were then defined:

- Take-Off (TO): $H = 0$ m, $M_0 = 0$ and $N_L = 1.05$ ($P = 100\%$).
- Top of Climb (TOC): $H = 10668$ m, $M_0 = 0.8$ and $N_L = 1$ ($P \approx 91\%$).
- Cruise: $H = 10668$ m, $M_0 = 0.8$ and $N_L = 0.95$ ($P \approx 82\%$).
- Low Power: $H = 10668$ m, $M_0 = 0.8$ and $N_L = 0.83$ ($P = 60\%$).
- Ground Idle: $H = 0$ m, $M_0 = 0$ and $N_L = 0.555$ ($P = 10\%$).

4.1. Model Validations

In order to verify the accuracy of the present model results, performance results for design point, off-design and transient simulations were compared with [7] performance results. Several parameters were considered for the validation process, with calculation of SFC and Ψ (specific thrust) for all models (and f for design point) and of relative spool speeds (N_L and N_H), T_{t4} and B for off-design and transient models.

The design point validation process was based on a parametric analysis with variation of design inputs such as the $T_{t4,R}$, $\pi_{HPC,R}$, $M_{0,R}$ and B_R. In a similar way, a parametric analysis of N_H, T_{t4} and flight conditions M_0 and H is followed with the off-design model. The transient model validation is performed with selected time-dependent inputs of fuel mass flow rate ($\dot{m}_{f,demand}(t)$) and power setting demand (and then of $N_{L,demand}(t)$).

Excellent agreement was verified when compared with GasTurb 12 [7] results for all models. With average relative errors not greater than 0.2% for design point validations and not greater than 0.6% for off-design computations. In transient calculations, the highest average relative error was verified for SFC calculation (for $\dot{m}_{f,demand}(t)$ deceleration simulation) with a respective value of 0.96%. Given the validation results obtained, the validity of the present model for performance calculations is confirmed. In Figures 3, 4 and 5, some validation examples are given for design point, off-design and transient SFC calculations, respectively.

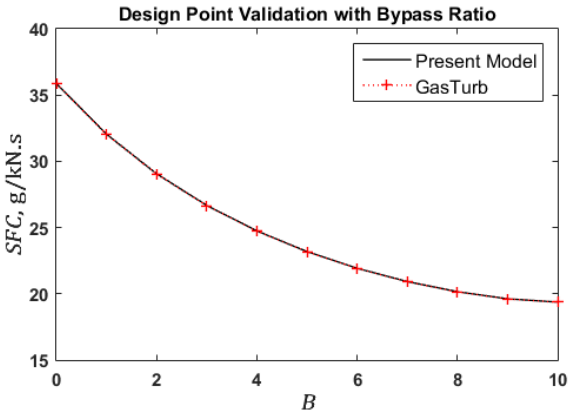

Figure 3: Design point validation of specific fuel consumption, SFC, with bypass ratio, B.

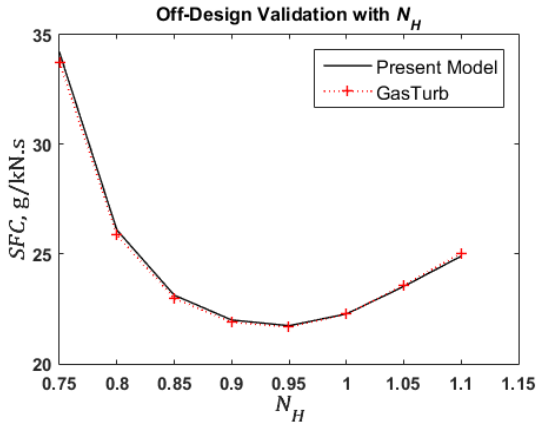

Figure 4: Off-design validation of specific fuel consumption, SFC, for given high-pressure relative spool speed, N_H.

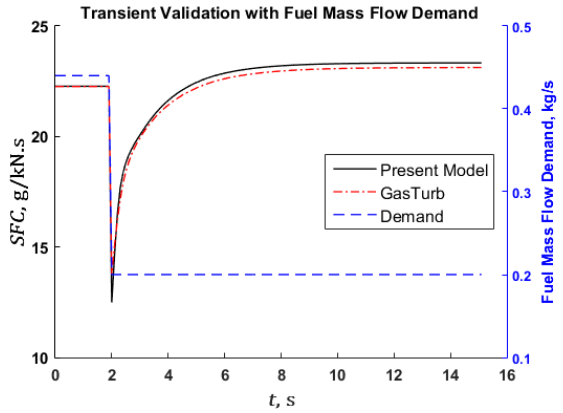

Figure 5: Transient validation of specific fuel consumption, SFC, with time, t, for $\dot{m}_{f,demand}(t)$ input (deceleration).

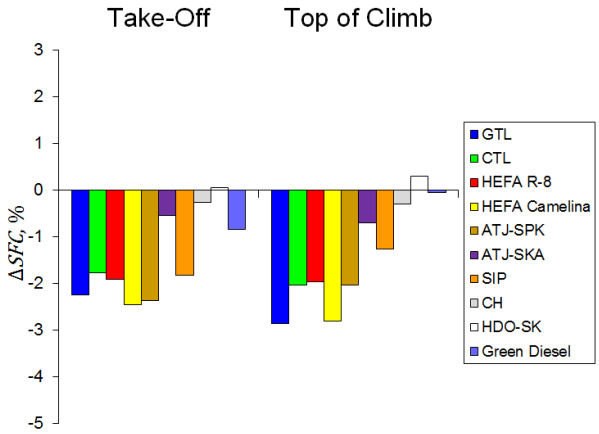

Figure 6: Summary of ΔSFC for Take-Off and Top of Climb operating conditions.

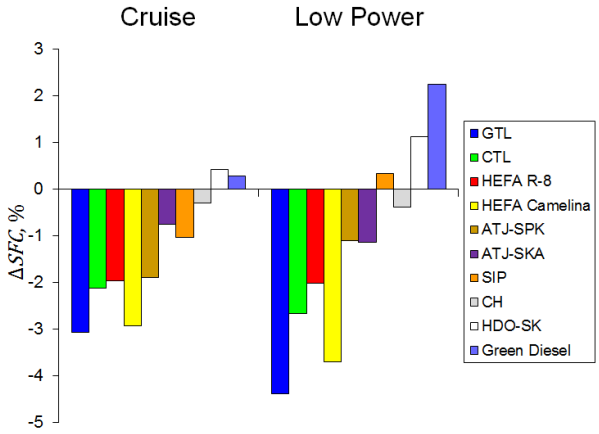

Figure 7: Summary of ΔSFC for Cruise and Low Power flight conditions.

4.2. Off-Design Performance Results

Taking advantage of the off-design model implemented, TO, TOC, Cruise and Low Power operating conditions were analysed. It was then verified that parameters such as T_{t4}, B and N_H are somewhat independent of the fuel burned. As expected, the most influenced performance parameters by fuel properties are the fuel mass flow rate, $\dot{m}_f$, and in a less extent the total thrust, F. Therefore, an analysis of the specific fuel consumption, SFC, is of significant relevance.

In Figures 6 and 7, the relative differences of specific fuel consumption for a certain fuel burning compared with Jet A-1, ΔSFC in %, are presented.

With this results, given that all alternative fuels present slightly higher values of net heat of combustion (up to 2.5% increase) compared with Jet A-1, fuels presenting worst atomization and evaporation qualities (higher viscosities, surface tensions and normal boiling points, mostly) with decrease of power setting (increase in combustion chamber loading) the combustion efficiency will decrease, until a point when a worse engine performance is verified. This result is clearly verified for fuels such as SIP, HDO-SK and Green Diesel. In general, alternative fuels may improve the engine performance in up to, approximately, 4% decreases in SFC.

Climbing at constant speed and $N_L = 1$ and TOC operation with varying Mach number were also simulated. The results obtained further confirmed the influence of the atomization and evaporation quality with the combustion chamber loading.

It was also possible to verify the performance results obtained for the maximum blending ratios, with Jet A-1, approved (referred to in section 1). For the cases of ATJ-SKA, CH and HDO-SK a maximum of 50% blending ratio was considered and Green Diesel with a ratio of 10% (based on SIP's ASTM approval). This approach confirmed that even with fuel blending, the specific fuel consumption can be decrease in up to 1.5%, for fuels such as GTL and HEFA Camelina (in this study).

4.3. Transient Performance Results

The transient simulations computed in the present work were defined through different types of input demands. From TOC initial condition, a fuel mass flow rate of 0.3 kg/s was demanded through a step input (deceleration). Then, considering power setting demand, from TOC conditions, a step decrease in power setting was demanded to a value of $P = 75\%$ (deceleration). For an acceleration response simulation, a demand of total thrust was simulated, from an initial thrust demand of 10.5 kN to 15 kN and Low Power initial flight conditions. For both power and thrust demand simulations, a proportional controller was used with gains of $C_P = 0.1$ and $C_P = 0.02$, respectively.

All transient simulations referred showcased negligible dynamic response differences, that is, delays and advances in responses of around 0.1 s were verified (which was the time step used).

However, through a simplified simulation of a fuel mass flow rate (corrected with pressure) control limit, the same acceleration simulation was performed (with thrust demand). As presented in Figure 8, alternative fuels presenting worse specific fuel consumption may delay the acceleration in approximately 2.7 s and 1.8 s (to reach demanded value) for Green Diesel and HDO-SK, respectively. Taking into account the time interval of thrust demand (15 s), these delays correspond to 18% and 12%, respectively, of the total simulation interval.

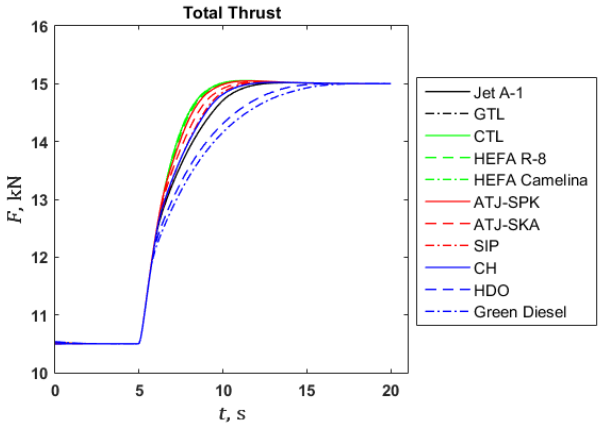

Figure 8: Total thrust, F, with elapsed time (acceleration), for fuel mass flow rate control.

4.4. Pollutant Emissions Results

For pollutant emissions results, TO, TOC, Cruise and Idle conditions are analysed. With the incorporation of the pollutant emissions model, NO_x, CO, UHC and soot emissions are computed with equations 10, 11, 12 and 13, respectively.

NO_x and soot pollutant emissions increase with power setting and CO and UHC increase with decrease in power setting. In Figure 9 and Figure 10, NO_x and soot, respectively, pollutant emissions relative to those obtained with Jet A-1, ΔEI_{NO_x} and ΔS in %, respectively, are presented for TO condition. In Figure 11 and Figure 12, CO and UHC pollutant emissions, respectively, relative to those obtained with Jet A-1, ΔEI_{CO} and ΔEI_{UHC} in %, respectively, are presented for the Idle operating condition.

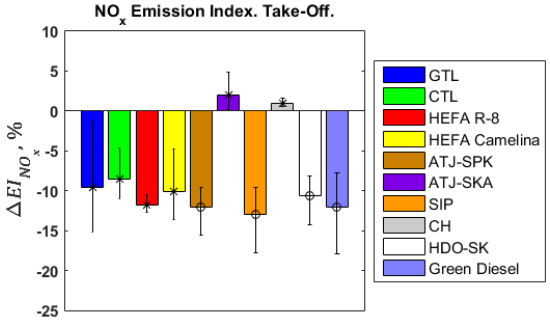

Figure 9: ΔEI_{NO_x} for Take-Off operating condition.

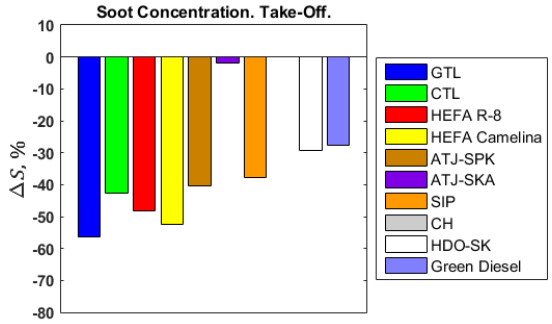

Figure 10: ΔS for Take-Off operating condition.

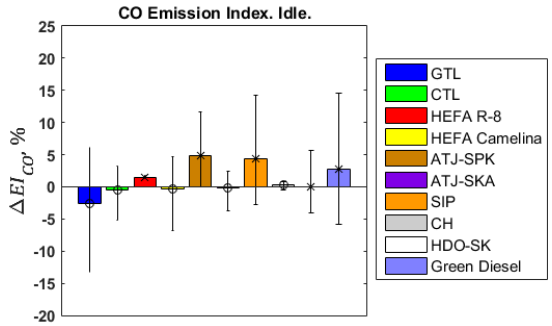

Figure 11: ΔEI_{CO} for Idle operating condition.

In Figures 9, 11 and 12, different markers are defined based on emissions dependence on evaporation. In cases where an "x" is plotted, with increase in evaporation time required (or decrease in combustion residence time) an increase in relative

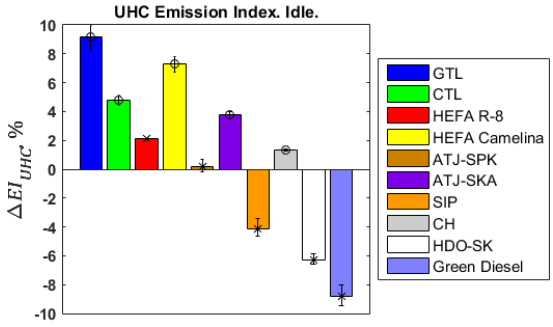

Figure 12: ΔEI_{UHC} for Idle operating condition.

pollutant emissions is verified, when compared to Jet A-1. For a circle marker, "o", the opposite occurs.

Through the analysis of computed NO_x pollutant emissions it is possible to verify that the burning of most alternative fuels may provide a significant decrease in NO_x emissions (more than 10% decrease).

Relative differences in CO pollutant emissions results showcase a higher dependence on fuel evaporation (and atomization). Therefore, it becomes relevant to analyse the tendency of CO emissions towards NO_x quantitative reduction. In fact, for a decrease in residence time (increase in evaporation time required), it is possible to verify that fuels with better atomization and evaporations qualities, such as FT-SPK, HEFA Camelina, ATJ-SKA and CH, will typically cause a reduction in CO pollutant emissions.

Relative differences in UHC pollutant emissions results, in turn, are only slightly dependent on the evaporation of the fuel droplet, with biggest influence arising from the fuel-air ratio employed in the primary zone. It follows that, considering if the fuel-air mixture in the primary zone is rich or lean, higher fuel-air ratios will typically decrease or increase the flame temperature, respectively. Which will mostly influence UHC emissions, where, as with CO, higher temperatures are preferred (the opposite occurring for NO_x emissions).

Although soot pollutant emissions calculations were based on a simple correlation and major simplifications were assumed (e.g. secondary zone parameters), the results obtained clearly state that, with most alternative fuels, a reduction in soot (smoke) will be possible (more than 50% reduction possible for TO). This result is mostly influenced by the fuel composition, where the lack of aromatics content is usually associated with a decrease in soot emissions [3].

With the present work, the influence of pollutant emissions differences with power setting was also verified. While NO_x emissions are not much influenced by power setting, but mainly by stoichiometric flame temperature differences, CO and UHC emission differences are significantly influenced by power setting. As previously stated, this will ultimately be related with fuel-air ratio changes, where typically in high power operating conditions (and if primary zone is rich), with improvements in SFC, CO and UHC emissions increase and the opposite otherwise. Soot pollutant emissions showcase better results with decrease in power setting, with influence of power setting highlighted in changes of fuel-air ratios and consequently on flame temperatures.

It should also be highlighted that, with a pollutant analysis for blending of fuels (as in subsection 4.2), good results in respect to NO_x and soot emissions, mainly, are obtained for most eligible drop-in fuels. As expected, all pollutant emissions deviations are decreased (with increase in Jet A-1 content), with a NO_x decrease in the order of 5% and soot in the order of 20%, for cruise conditions and most fuels.

Based on the pollutant results obtained with the present model, a comparison with selected literature results was followed, showing good overall agreement.

5. Conclusions

In order to evaluate the performance and environmental impact of alternative jet fuel burning, a simple aero-engine turbofan 0-D model was implemented. Enabling the study of different operating conditions, a design and off-design model was developed, along with a transient model.

The implemented models and results obtained were validated (based on literature or on GasTurb 12 performance results), showcasing an overall good agreement.

From the analysis of the performance results obtained in the present work, it is possible to conclude that most of the alternative fuels considered may improve the engine performance (specific fuel consumption) when compared with conventional jet fuel burning. In this regard, the net heat of combustion of the fuel plays a major part as well as the atomization and evaporation quality, with influence mainly visible with variation of power setting. In an overall perspective, fuels that may be viewed as better options (thermodynamically) compared with Jet A-1 are FT-SPK, HEFA-SPK, ATJ-SPK, ATJ-SKA and CH fuels. It should be noted as well that, a decrease in fuel consumption results in a decrease in greenhouse gases emissions such as CO_2 and H_2O (products of complete combustion).

Although small discrepancies were verified in all transient simulations performed, considering fuel mass flow control, fuel impact on transient response is evidenced. In fact, as previously referred, fu-

els such as HDO-SK or Green Diesel may require a significant additional time to achieve demanded operating conditions, which may compromise flight safety.

In an environmental analysis, through NO_x, CO, UHC and soot pollutant emissions estimations from empirical correlations (Rizk & Mongia, 1994), it was possible to conclude that alternative fuels properties will mostly influence soot emissions (despite its high complexity). In fact, for all flight conditions, typically, the burning of alternative fuels will result in a decrease in soot emissions. This is mostly associated with the lower aromatic content of the alternative fuels considered.

For the case of NO_x pollutant emissions, excluding fuels such as ATJ-SKA and CH, overall good results, with decrease in pollutant emissions is verified. These results are mostly a function of the differences in stoichiometric flame temperature. For CO pollutant emissions, on the other hand, typically a result of incomplete combustion, an higher atomization and evaporation dependence is verified. One can conclude that with a decrease in combustion residence time (ideal for NO_x emissions), most fuels, such as GTL and CTL, HEFA-SPK (Camelina), ATJ-SKA and CH, may reduce considerably CO pollutant emissions in a wide range of flight conditions, due to faster evaporation. Finally, with UHC pollutant emissions calculations it is possible to conclude that they are mostly influenced by the fuel-air ratio employed, affecting the flame temperature calculation (with lower temperatures preferred).

Fuels such as ATJ-SKA and CH, showcase similar results and in some situations improved results in comparison with Jet A-1, which is regarded as a significant step towards neat alternative fuel wide-scale use, substituting conventional kerosene.

With the present work, it is possible to conclude that the combustion of most alternative fuels being developed and already certified may ultimately result in an overall performance enhancement, with an associated decrease in greenhouse gases emissions, as well as a significant decrease of undesired pollutant emissions (mostly soot), depending on the operating condition. Acknowledging, in addition, the associated better overall life cycle emissions of CO_2 for sustainable alternative fuels production pathways, the sustainable future of the aviation industry is considered as secured and shall be only dependent on the costs of fuels and support given by policymakers towards the sustainable alternative fuels pathway growth.

Acknowledgements

The author would like to thank Prof. Dr. João Manuel Melo de Sousa for his continuous and invaluable support, assistance and constructive criticism during the present work.

References

[1] International Civil Aviation Organization, *ICAO Environmental Report 2013, Aviation and Climate Change*, 2013.

[2] International Air Transport Association, *IATA Sustainable Aviation Fuel Roadmap*, 1st Edition, 2015.

[3] Lefebvre, A., and Ballal, D., *Gas Turbine Combustion: Alternative Fuels and Emissions*, 3rd Edition, CRC Press, 2010.

[4] Rizk, N., and Mongia, H., "Emissions Predictions of Different Gas Turbine Combustors", *AIAA Paper 94-0118*, 1994.

[5] Walsh, P., and Fletcher, P., *Gas Turbine Performance*, 2nd Edition, Blackwell Science, 2004.

[6] Mattingly, J., *Elements of propulsion: Gas Turbines and Rockets*, 2nd Edition, AIAA Education Series, American Institute of Aeronautics and Astronautic, 2006.

[7] Kurzke, J., *GasTurb 12: Design and Off-Design Performance of Gas Turbines*, GasTurb GmbH, 2015.

[8] Zschocke, A., Scheuermann, S., and Ortner, J., "High Biofuel Blends in Aviation (HBBA)", Lufthansa and WIWeB Interim Report ENER/C2/2012/420-1, 2015.

[9] Cohen, H., Rogers, G., and Saravanamuttoo, H., *Gas Turbine Theory*, 4th Edition, Longman Group Limited, 1996.

[10] Riazi, M., *Characterization and Properties of Petroleum Fractions*, 1st Edition, American Society for Testing and Materials (ASTM), 2005.

[11] Gülder, Ö. L., "Flame Temperature Estimation of Conventional and Future Jet Fuels", *Journal of Engineering for Gas Turbines and Power*, 108, 376-380, 1986.

[12] Chin, J., and Lefebvre, A., "Steady-State Evaporation Characteristics of Hydrocarbon Fuel Drops", *AIAA Journal*, 21(10), 1437-1443, 1983.

[13] Bräunling, W., *Flugzeugtriebwerke - Grundlagen, Aero-Thermodynamik, Ideale und reale Kreisprozesse, Thermische Turbomaschinen, Komponenten, Emissionen und Systeme*, 4th Edition, Springer-Verlag, 2015.